

Considerations In the Development of the Advanced Propagation Model (APM) For U.S. Navy Applications

Amalia E. Barrios
SPAWARSSYSCEN SAN DIEGO (SSC San Diego)
Atmospheric Propagation Branch, Code 2858
49170 Propagation Path
San Diego, CA 92152-7385

I. INTRODUCTION

THE Navy Radio and Sound Laboratory was originally built in San Diego during World War II to study radiowave and underwater acoustic propagation effects. The laboratory has grown over the years and has undergone many organizational and name changes since then to become what is currently the Space and Naval Warfare Systems Center San Diego (SSC San Diego). What is now the Atmospheric Propagation branch at SSC San Diego has been in the business of researching and modeling effects due to atmospheric conditions on radiowaves since the 1940's.

Primarily funded by the U.S. Navy, much of the work we do in the Atmospheric Propagation branch has been not only in the propagation research area but also in the development of applications displays and assessment tools specifically for use by the U.S. Navy. However, a software package with the fanciest GUI wrapped around the most scientifically accurate propagation model in the world will not be used by many if the model executes slowly. Therefore, we spend a great deal of effort in designing an efficient model, automating much of the input parameters needed to get meaningful results from the model.

This paper will focus primarily on the Advanced Propagation Model (APM), developed by the Atmospheric Propagation branch at SSC San Diego, and looks at initial developments of the model along with approximations made in its design for consideration of the operational user.

II. BACKGROUND

It is assumed the reader has a basic understanding of some of the terminology commonly used in meteorology and propagation modeling. Although brief descriptions and definitions are given below, for more detailed information the reader should refer to [1] and [2] - two very good references on the subject.

A. Propagation Factor and Loss Definition

In all radiowave propagation models, the basic quantity computed is the propagation factor F . The propagation factor is defined as

$$F = \left| \frac{E}{E_0} \right|, \quad (1)$$

where E is the field strength at a point, including antenna pattern effects but normalized to unity gain antennas, and E_0 is the field strength that would occur at that point under free space conditions if loss-free isotropic antennas were used for both the transmitter and receiver [1]. Once F is computed, propagation loss in dB is determined by taking the difference between the free space loss and F (in dB). In equation form:

$$L = 20 \log \left(\frac{4\pi r}{\lambda} \right) - 20 \log F. \quad (2)$$

The first term in (2) is the free space loss, where r is the range and λ is the wavelength. We make the distinction between propagation loss and transmission loss because by definition, propagation loss includes antenna pattern effects but does not include the gain of the antennas (i.e., normalized to unity gain), whereas transmission loss includes both.

From (2) it should be apparent that F contains all environmental affects on the emitted electromagnetic (EM) wave. This includes effects from the atmosphere and a variable reflecting surface, such as rough ocean or land.

B. Standard and Nonstandard Refractive Conditions

The term "standard atmosphere" refers to the condition when EM waves bend downward with a curvature approximately $\frac{4}{3}$ that of the earth's radius. The most dramatic propagation anomalies usually occur over water where atmospheric ducting is more significant and consistent than over land [1]. A vertical refractivity profile is defined by a series of modified refractivity (M-unit) values that vary in height:

$$M(z) = \left(n - 1 + \frac{z}{a} \right) \times 10^6. \quad (3)$$

Here, z represents height, n is the index of refraction, and a is the earth's radius.

Ducting conditions occur when a trapping layer (negative M-unit gradient) exists in a vertical refractivity profile. The three basic ducting mechanisms are evaporation, surface-based, and elevated ducts. It is the presence of these ducts that affect radar and communications performance as evidenced by increased or decreased detection and communication ranges. Atmospheric ducts act as a leaky waveguide, thereby trapping radiated energy and propagating EM waves far beyond the normal horizon range. Because of this trapping effect, at altitudes just above

Report Documentation Page				Form Approved OMB No. 0704-0188	
Public reporting burden for the collection of information is estimated to average 1 hour per response, including the time for reviewing instructions, searching existing data sources, gathering and maintaining the data needed, and completing and reviewing the collection of information. Send comments regarding this burden estimate or any other aspect of this collection of information, including suggestions for reducing this burden, to Washington Headquarters Services, Directorate for Information Operations and Reports, 1215 Jefferson Davis Highway, Suite 1204, Arlington VA 22202-4302. Respondents should be aware that notwithstanding any other provision of law, no person shall be subject to a penalty for failing to comply with a collection of information if it does not display a currently valid OMB control number.					
1. REPORT DATE 14 APR 2005		2. REPORT TYPE N/A		3. DATES COVERED -	
4. TITLE AND SUBTITLE Considerations In the Development of the Advanced Propagation Model (APM) For U.S. Navy Applications				5a. CONTRACT NUMBER	
				5b. GRANT NUMBER	
				5c. PROGRAM ELEMENT NUMBER	
6. AUTHOR(S)				5d. PROJECT NUMBER	
				5e. TASK NUMBER	
				5f. WORK UNIT NUMBER	
7. PERFORMING ORGANIZATION NAME(S) AND ADDRESS(ES) SPAWARSSYSCEN SAN DIEGO (SSC San Diego) Atmospheric Propagation Branch, Code 2858 49170 Propagation Path San Diego, CA 92152-7385				8. PERFORMING ORGANIZATION REPORT NUMBER	
9. SPONSORING/MONITORING AGENCY NAME(S) AND ADDRESS(ES)				10. SPONSOR/MONITOR'S ACRONYM(S)	
				11. SPONSOR/MONITOR'S REPORT NUMBER(S)	
12. DISTRIBUTION/AVAILABILITY STATEMENT Approved for public release, distribution unlimited					
13. SUPPLEMENTARY NOTES See also ADM001798, Proceedings of the International Conference on Radar (RADAR 2003) Held in Adelaide, Australia on 3-5 September 2003., The original document contains color images.					
14. ABSTRACT					
15. SUBJECT TERMS					
16. SECURITY CLASSIFICATION OF:			17. LIMITATION OF ABSTRACT UU	18. NUMBER OF PAGES 6	19a. NAME OF RESPONSIBLE PERSON
a. REPORT unclassified	b. ABSTRACT unclassified	c. THIS PAGE unclassified			

the duct height there exists a “radar hole” in which propagation loss is much higher (or signal strength is greatly decreased) than under standard atmospheric conditions. Of course, nonstandard conditions do not necessarily mean ducts are present. Subrefractive or superrefractive conditions can also arise causing a decrease (subrefractive) or an increase (superrefractive) in detection range. Fig. 1 illustrates the effects from different types of atmospheric conditions.

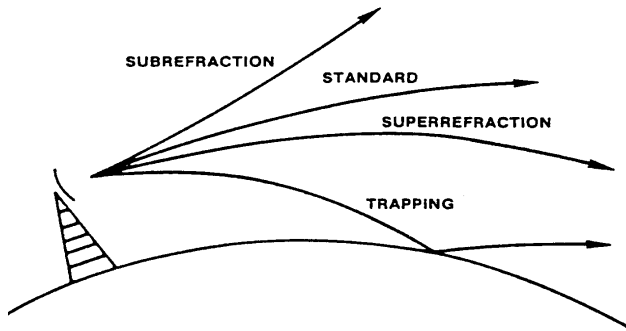


Fig 1. Various refractive conditions.

Since our end customer is the U.S. Navy, for many years our focus has been in studying propagation effects due to nonstandard atmospheric conditions that are prevalent over the ocean. It was only in the last 10 years that we have begun to investigate and model effects due to variable terrain. The evaporation duct, the most persistent ducting mechanism over water, is non-existent over land. Although in general the formation of surface-based and elevated ducts are less consistent over land, a common occurrence is the formation of small surface-based ducts over desert terrain. The formation of these ducts closely follows a diurnal variation as they form nightly due to dissipation of heat from the desert floor.

Only a limited frequency range within the radiowave spectrum is affected by nonstandard atmospheric conditions mentioned above. Therefore, we are not concerned with modeling propagation effects over the entire radiowave spectrum but deal with only those frequencies that are affected by refractive conditions in the troposphere – mainly the frequency range between 100 MHz and 20 GHz. Below 100 MHz the dominant propagation mechanisms are the surface wave and sky wave due to the ionosphere. Above 20 GHz scattering and gaseous absorption are dominant. Although anomalous refractive conditions can still affect radiowaves at higher frequencies, say at 94 GHz, absorption and attenuation due to rough surfaces counteract any trapping effects due to ducting [1].

As a final note, APM does not include any meteorological models. The proper information necessary to feed *any* propagation model is ultimately what is important, but strictly speaking, APM models the effects from the medium but does not model the propagating medium itself. For upper air information the refractivity profile is obtained by direct measurement via radiosondes or rocketsondes. There are several bulk models that are commonly used to compute evaporation duct profiles from bulk meteorological

measurements [3], however, any meteorological modeling is done external to APM. All environmental information needed to adequately compute propagation loss over sea or land are treated as inputs to the model. Therefore it is assumed that, however obtained, the profile and terrain information are known upon running APM. Terrain information is readily available through various databases such as the Digital Terrain Elevation Database (DTED) and the United States Geological Survey (USGS).

III. INITIAL DEVELOPMENTS

The first propagation model developed by SSC San Diego (then known as the Naval Ocean Systems Center, NOSC) for shipboard operational use is FFACTOR, which is the internal computational engine for the Integrated Refractive Effects Prediction System (IREPS) EM assessment software package. IREPS has been in wide use by the U.S. Navy since the mid 1970s [4].

Designed specifically for over-water applications, FFACTOR accounts for standard and nonstandard refraction, reflection over smooth and rough ocean surfaces, diffraction, and troposcatter. FFACTOR is somewhat limited as horizontal homogeneity of the refractive profile is assumed, field strength is computed only for surface-based platforms, and no terrain effects are considered. However, for the operational needs of the Navy during this time, IREPS was very effective as a tactical decision aid. The Cold War had not yet ended and the Navy was not as concerned with the littoral environment then as it is now, so the absence of terrain effects in the propagation model was not a great deterrent to its use or its usefulness. Over the sea the troposphere usually exhibits horizontal homogeneity over long distances. It has been found that the assumption of a horizontally stratified troposphere leads to valid operational propagation assessments 86% of the time [5]. In fact, the use of IREPS coverage diagrams in strike warfare flight profile selection has been verified operationally to be effective 85% of the time for *open ocean* conditions.

In coastal areas the environment can change drastically at air/mass boundaries associated with wave cyclones and land/ocean interfaces [6]. With Navy operational requirements focusing on the littoral environment in the last decade or so, there was a strong need to accommodate range-dependent refractive profiles, along with terrain effects, in the propagation model.

Already in widespread use in the acoustic community, in 1989 we adopted the split-step Fourier parabolic equation (PE) algorithm for our EM applications as the technique allowed for a range-varying propagating medium. The PE method, developed by Hardin and Tappert [7], is accurate, robust, and more efficient than equally sophisticated methods. The novel approach of using Fast Fourier Transforms (FFTs) to “march”, or propagate, the field solution in range at many different receiver heights simultaneously, provided a relatively fast technique to produce coverage diagrams for use as tactical decision aids.

Typical coverage areas for Navy applications such as long-range air-search radars, surface-search radars, and surface-to-air or air-to-air communications are roughly 10 km in height by 300-400 km in range. Although the PE

algorithm is relatively efficient when compared to other equally accurate techniques, the fundamental limitation to its practical use as an operational model is the size of the FFTs needed to accommodate these coverage areas. There is also an inherent limitation [within the PE approximation] in the size of the propagation angle it can accommodate.

Figure 2 shows a loss diagram for a typical coverage area using a 3 GHz radar over a sea/land path in the presence of a surface-based duct. For illustration purposes, this coverage

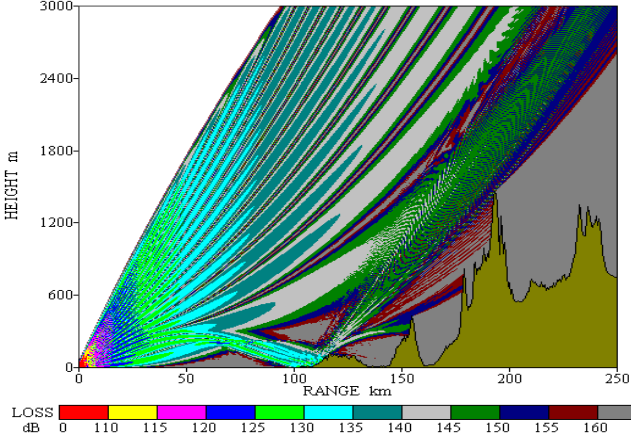


Fig. 2. Coverage diagram for 3 GHz and surface-based duct.

diagram was produced using the PE model with a fixed maximum PE angle. The region in the diagram corresponding to propagation angles beyond the maximum PE limit is indicated by the white area in the upper left. For practical applications, this coverage “gap” is not a hindrance for most propagation modelers as most of the effects of interest are at low altitudes and long ranges. However, the operational user who is not familiar with any of the caveats of the PE algorithm (nor should they be!) views this “gap” as a weakness in their radar or communications coverage. Indeed, there have been some instances where operational users believed an aircraft could fly at a higher altitude and “sneak” in undetected within this coverage gap! Therefore, the toughest requirement in producing a useable coverage diagram for the operational user is computing loss at *all* heights and ranges within the desired coverage area to eliminate any confusion.

It was the realization that a stand-alone PE model could not provide loss predictions over extremely high angles at close ranges, along with the numerically intensive calculations required [for large heights] for normal radar applications mentioned above, that led to the development of a hybrid ray optics/PE model. Developed by Herb Hitney at SSC San Diego (then NRaD), the Radio Physical Optics (RPO) model was the first EM propagation model to combine a high fidelity PE algorithm with simpler ray optics and flat earth models [8]. The “hybridization” within RPO resulted in a very efficient high fidelity model that has now been in use by the operational and scientific community since its release in 1992 [9].

RPO was developed strictly for use on over-water applications, therefore, a separate PE model that could also account for terrain effects was developed shortly after, called the Terrain Parabolic Equation Model (TPEM). TPEM was developed as a stand-alone PE model [10] and

was maintained in parallel with RPO.

With new and improved propagation models RPO and TPEM, it became apparent that maintaining two separate models for any kind of software system integration would be cumbersome, primarily because of the many parallels between the two models. Therefore, with the development of our new and improved EM assessment capability, the Advanced Refractive Effects Prediction System (AREPS), we thought it was a logical step to combine the strengths and capabilities of both RPO and TPEM into one propagation model. This model is called the Advanced Propagation Model (APM).

IV. ADVANCED PROPAGATION MODEL

APM contains the same hybridization methods internal to RPO, consisting of four basic submodels. These are flat earth (FE), ray optics (RO), extended optics (XO), and the split-step Fourier PE algorithm. It is the PE algorithm that is the primary model for which the other three submodels are built around.

The PE model is undoubtedly more capable than the other three in computing loss due to varying refractivity and terrain along the propagation path. Therefore, all parameter constraints and initializations are performed for the PE algorithm first, keeping the region over which it is applied to a minimum for the most efficiency. The other three models are then used to compute loss in regions where the PE algorithm is not applied. Figure 3 shows a diagram of the typical regions for a given coverage area over which each model is applied. The following sections will describe in more detail each of the models and their regions of applicability.

A. Parabolic Equation Model

The basic PE formulation, using the wide-angle propagator, is given as

$$u(x + \Delta x, z) = e^{ik_0 \Delta x 10^{-6} M(z)} \mathbf{F}^{-1} \left\{ e^{i \Delta x \sqrt{k_0^2 - p^2} - k_0} \mathbf{F} \{ u(x, z) \} \right\} \quad (4)$$

where x and z represent the Cartesian range and height coordinates, respectively, k_0 is the free space wavenumber ($2\pi/\lambda$), Δx is the incremental range step over which the field

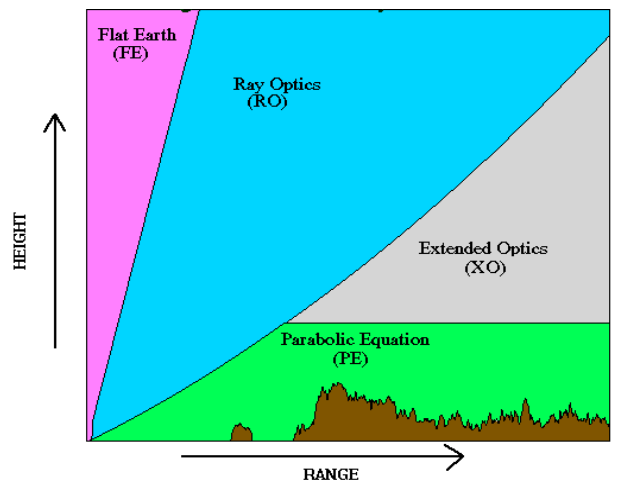


Fig. 3. Regions of APM hybrid submodels.

solution is propagated, $M(z)$ is the height-varying refractive profile, and \mathbf{F} and \mathbf{F}^{-1} represent the forward and inverse Fourier transforms, respectively. The transform variable p is equal to $k_0 \sin \vartheta$, ϑ being the propagation angle referenced from the horizontal. The quantity u is a scalar component of the electric field and in the process of normalizing and converting from spherical to Cartesian coordinates the field retains an explicit range dependence where we now compute the propagation factor F as

$$F = |u(x, z)| \sqrt{x}, \quad (5)$$

or in dB,

$$20 \log F = 10 \log [(u_r^2 + u_i^2) x]. \quad (6)$$

In (6) u_r and u_i are the real and imaginary components of $u(x, z)$, respectively. Equation (6) is then used in (2) to compute the propagation loss. There are numerous references in the literature on the derivation of (4), however, the reader is referred to [10-12] for the most recent.

Most of the number-crunching within the PE algorithm is done by the FFTs. Therefore, in order to get the most efficiency we've constrained the model to run with the smallest FFT size possible. Analogous to signal processing methods where one deals with signals in time and frequency domains, here we have the EM field specified in the height (z -space) and angle (p -space) domains. The grid or height bin size follows the Nyquist criteria and is determined by

$$\Delta z = \frac{\lambda}{2 \sin \vartheta_{\max}}. \quad (7)$$

The maximum propagation angle ϑ_{\max} corresponds to the "bandlimit" for the transform variable p . From (7) it can be seen that for a given wavelength, minimizing ϑ_{\max} will maximize Δz and a smaller FFT size can then be used to compute loss up to a specified height. Of course, there are more issues to consider in the implementation of the PE algorithm, such as the types of filters used for the FFTs to avoid aliasing, the size of the filter region, how often to filter, etc., which will all affect the final determination of ϑ_{\max} , and hence, Δz . However, this is the general rule made within APM: for a given refractivity and terrain profile, the minimum propagation angle and height necessary to encompass all refractive effects and the *majority* of terrain effects are determined first, then (7) is used to define the grid size and FFT size needed.

Even the strongest surface-based ducts trap radiowaves at propagation angles only to within 1° . Therefore, for over-water applications the minimum propagation angle necessary to encompass any and all refractive effects need not be large. When including terrain effects, however, some compromises must be made.

To produce optimum results, the PE algorithm as implemented in APM, should not be run with a propagation angle less than some minimum angle. This minimum angle varies depending on frequency and is determined from a polynomial fit of a set of angles vs. frequencies that were initially determined by trial and error. As an example, at the lowest frequency of 100 MHz, the minimum PE angle may be as much as 5° whereas at 20 GHz the minimum angle may be less than 0.4° .

The maximum propagation angle is determined via an iterative geometric ray trace from the transmitter height to 120% of the maximum terrain height along the propagation

path, or the height of the highest trapping layer specified in the refractivity profile(s), whichever is greater. ϑ_{\max} is then the larger of this angle determined from ray trace, and the minimum angle determined from the polynomial fit mentioned in the previous paragraph.

In the initialization of the ray trace, the starting launch angle, ψ , corresponds to the limiting grazing angle defining the maximum range and altitude for which the RO method can be applied. The limiting grazing angle is 2.5 times the limit given by Reed and Russell [13], limited to values above 0.002 radians, and includes an extra term to account for ducting:

$$\psi = \psi_0 + \delta\psi; \quad \psi_0 = \text{MAX} \left(.002, \frac{.04443}{f_{\text{MHz}}^{0.333}} \right), \delta\psi = \sqrt{2 \times 10^{-6} \Delta M}. \quad (8)$$

In (8), f_{MHz} is the frequency in MHz and ΔM is the M-unit difference in the refractive profile between the minimum value and that at the surface. For range-dependent profiles ψ_0 in (8) is doubled.

Once ϑ_{\max} is determined, Δz is obtained from (7) and the FFT size can be easily determined according to the height that's required for the PE calculation domain (as mentioned above and used in the ray trace iteration). The PE algorithm is then applied using (4).

For finite conducting or rough surface boundaries the Discrete Mixed Fourier Transform (DMFT) is used [14]. The DMFT algorithm will not be described here as the reader can refer to [14] for a more detailed description. However, the algorithm does contain an implicit numerical instability for cases when the real portion of the impedance term approaches zero. The DMFT as described in [14] solves for the boundary condition in terms of a central difference formulation. Recently, a new formulation of the DMFT, in which a backward difference form is proposed, seems to have corrected this instability [15].

Equation (4) is the general PE algorithm for propagation over smooth earth. In computing loss over terrain, there is a rigorous form of the PE algorithm described in [10] and [12], however, in this rigorous form the maximum PE propagation angle depends heavily on the maximum slope of the terrain along the path. For any general terrain profile that one would encounter in nature, a propagation model based on this form of the PE would be very restrictive as angles could approach upwards of 90° . In keeping with the goal of developing an efficient model for operational use, the PE algorithm used to account for terrain effects [in APM] remains as shown in (4) but the field is adjusted according to the "boundary shift" method described in [16].

The idea behind the boundary shift method is simple. The terrain elevation is approximated at each PE range step by an *integer* number of height bins, N_t . If T_x is the actual terrain elevation, then N_t is determined according to

$$N_t = \frac{T_x}{\Delta z}, \quad (9)$$

such that

$$T_x - N_t \Delta z < \Delta z. \quad (10)$$

The field is then shifted in z -space downward by N_t bins for a positive terrain slope and upward for a negative slope. The field is then set to equal to zero for those bins that remain at

the top or bottom of the FFT grid. This is illustrated in Fig. 4, where $nfft$ is the FFT size and u_i represents the i^{th} bin of the complex scalar field in z -space: $u_i = u(x, i \Delta z)$.

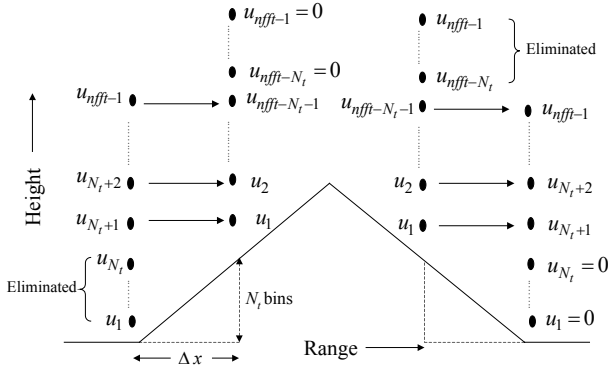


Fig. 4. Boundary shift method in APM.

The boundary shift method was arrived at not based on any sound mathematical or physical formulation, but on intuitive concepts and approximations to the more accurately obtained field via the coordinate transformation described in [10] and [12]. As shown in [16], the resulting predicted diffraction loss did not differ greatly from the more rigorously obtained values. Effectively, what the boundary shift method fails to account for is high-angle energy that is reflected off the ground surface. Since most natural terrain surfaces are poor reflectors (unlike the ocean) this is not a poor approximation for surface-to-air applications over land, as shown by an independent operational analysis study [17].

B. Ray Optics Model

The RO model is applied at angles above the maximum PE propagation angle, \mathcal{Q}_{max} , and below 5° . The RO method consists of tracing a series of direct and reflected rays through selected control points, and then interpolating the magnitudes of these rays and the phase angle between them at each desired receiver point. The magnitude of each ray is computed from a spreading term relative to free space spreading, and the phase angle is determined from the optical path length differences from the ground range for each ray [8].

The range, spreading, and optical path length difference are computed at each ray trace step i . These are then summed over the entire ray path for each ray once the desired receiver point is reached and are given by

$$X = \sum_i (\alpha_1 - \alpha_0) g_i^{-1}, \quad S = \sum_i \left(\frac{\alpha}{\alpha_1} - \frac{\alpha}{\alpha_0} \right) g_i^{-1},$$

$$D = \sum_i \left[(10^{-6} M_i - \frac{1}{2} \alpha_0^2) (\alpha_1 - \alpha_0) + \frac{1}{3} (\alpha_1^3 - \alpha_0^3) \right] g_i^{-1}, \quad (11)$$

$$g_i = \frac{10^{-6} (M_{i+1} - M_i)}{z_{i+1} - z_i}.$$

In (11) α is the elevation angle at the transmitter, and α_0 and α_1 are the angles at the beginning and end, respectively, of each ray trace step. These are obtained by the standard geometric ray trace formulas based on small angle approximations to Snell's law. Once the total range, X , spherical spreading, S , and total optical path length difference, D , have been computed for each ray the

propagation factor for the direct and reflected rays, F_d and F_r , are given by

$$F_d^2 = f_d^2 \left| \frac{X}{\beta_d S_d} \right|, \quad F_r^2 = f_r^2 R^2 \left| \frac{X}{\beta_r S_r} \right|, \quad (12)$$

$$\Omega = (D_r - D_d) k_0 + \varphi.$$

In (12) f_d and f_r are the antenna pattern factors for the direct and reflected ray elevation angles, respectively, at the transmitter. β_d and β_r are the propagation angles at the receiver point for the direct and reflected rays, R and φ are the magnitude and phase lag of the Fresnel reflection coefficient, and Ω is the total phase angle between the direct and reflected rays. The propagation factor F of the resultant field between both rays can now be computed using

$$F^2 = F_d^2 + F_r^2 + 2 F_d F_r \cos \Omega. \quad (13)$$

A basic limitation of the RO model is that it assumes a horizontally homogeneous refractive environment and must be used over a flat surface in regions where it is applied, thereby requiring terrain profiles to be flat within the first few kilometers from the source. For terrain profiles that vary at all ranges, coverage diagrams produced are limited in angle so loss will not be computed at large heights and near ranges.

C. Flat Earth Model

The FE model is applied at all heights and ranges up to 2.5 km from the source (assuming the terrain profile is flat for the first 2.5 km) and is applied at all propagation angles greater than 5° . Although F is computed based on flat earth geometry, earth curvature and refractive effects are still accounted for in order to ensure smooth transitioning between the FE and RO regions at extremely high altitudes and ranges. This is done by using an effective earth's radius factor, k_e , which is computed by ray trace using an elevation angle of 5° from the source to the maximum height of interest. The propagation factor F is then computed using (13) with the following substitutions:

$$z_e = z - \frac{x^2}{2ak_e},$$

$$r_1 = \sqrt{(z_e - z_t)^2 + x^2}, \quad r_2 = \sqrt{(z_e + z_t)^2 + x^2}; \quad (14)$$

$$\alpha_d = \tan^{-1} \left[\frac{(z_e - z_t)}{x} \right], \quad \alpha_r = -\tan^{-1} \left[\frac{(z_e + z_t)}{x} \right];$$

$$\Omega = (r_2 - r_1) k_0 + \varphi; \quad F_d^2 = f(\alpha_d)^2; \quad F_r^2 = f(\alpha_r)^2 R^2.$$

In (14), r_1 and r_2 are the direct and reflected ray path lengths, respectively, x is the ground range, and a is the mean earth's radius. It should be noted that in this region the free space loss should be computed using the slant range, not ground range. Therefore, in determining propagation loss, r should be replaced with r_1 in (2).

D. Extended Optics Model

The XO model is applied at all heights above the maximum height of the PE region, where the refractive environment consists of positive linear gradients only. The XO method is based on the parallel ray assumption of direct and reflected rays from surface-based emitters. Namely, for long ranges and high altitudes, the propagation angles for both direct and reflected rays are assumed to be parallel to a

first order approximation and the resultant field can be considered constant for a given propagation angle.

The outgoing propagation angle at the top of the PE region is determined at each range step via spectral estimation and this angle is then used to “extend” F (which is known from the PE solution) outward via simple ray tracing methods. For over-water applications this is a very good assumption as shown for various cases in comparison to more rigorous propagation models [1]. Over terrain, this is less so.

Figure 5(a) shows a coverage diagram using both PE and XO models. The black horizontal line indicates where the top of the PE region ends and the XO region begins. Fig. 5(b) shows a height vs. loss plot for a receiver range of 175 km for the case in Fig. 5(a). In Fig. 5(b) a comparison is shown between loss values computed using only the PE model for the entire maximum height of the coverage diagram (shown in red) and that computed using the XO model (shown in black). Since only the magnitude (i.e., F) is extended and not the phase of the field, there is of course some discrepancy between the two. However, for practical considerations the method can still be used for operational assessments as the strongest lobing features are accounted for, even though the fine scale interference features are not.

V. FINAL COMMENTS

With the exception of the PE model all of the methods described in Section IV are applicable only for surface-based emitters. For airborne applications a combination of the PE and FE submodels are used where the PE model is run with a value for \mathcal{G}_{max} of no less than 5° . Above this angular PE limit the FE model is applied, but the computation of F is only done for the direct ray. At such high altitudes and angles any fine scale lobing structure will vary about the mean, or free space loss value; therefore considering only the direct ray component in this region is sufficient for most operational applications.

While it is obvious that many approximations have been made in the interest of speed over fidelity, we feel that many of these do not greatly compromise the overall accuracy of APM. These approximations are only considered for implementation within APM when favorable comparisons are made against a more rigorous propagation model. The techniques and methods described in Section IV have been extensively tested and validated over the years by not only SSC San Diego but also by Navy operations personnel. Although we have always emphasized that APM is an operational model, it has also performed quite well when used in scientific studies by independent researchers.

REFERENCES

- [1] H.V. Hitney, “Refractive Effects from VHF to EHF: Propagation Mechanisms”, in *Propagation Modelling and Decision Aids for Communications, Radar and Navigation Systems*, AGARD Lecture Series 196, Sept. 1994, pp. 4A-4B.
- [2] D.E. Kerr, *Propagation of Short Radio Waves*, New York, McGraw-Hill, 1951.
- [3] L.T. Rogers and R.A. Paulus, “Measured Performance of Evaporation Duct Models,” *Proc. Of the 1996 Battlespace Atmospherics Conference*, NRaD TD 2938, 3-5 Dec 1996, pp 273-281.
- [4] H.V. Hitney and J.H. Richter, “Integrated Refractive Effects Prediction System,” *Naval Eng. J.*, vol. 88, no. 2, April 1976, pp 257-262.

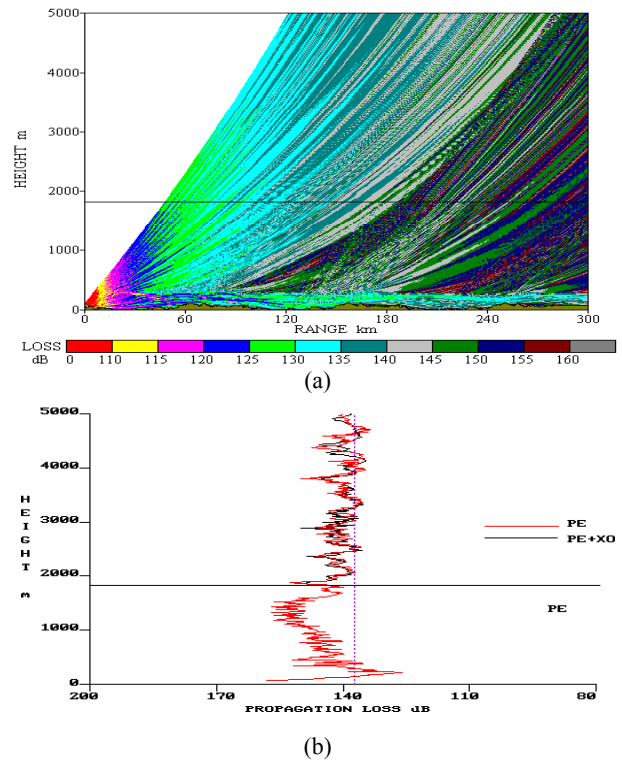


Fig. 5. Coverage diagram with low-lying variable terrain and 300 m surface-based duct for a transmitter at 1 GHz, antenna height at 25 m (a). PE vs. XO values from (a) at 175 km receiver range (b).

- [5] H.V. Hitney, J.H. Richter, R.A. Pappert, K.D. Anderson, and G.B. Baumgartner, Jr., “Tropospheric radio propagation assessment,” *Proc. IEEE*, vol. 73, pp. 265–285, Feb 1985.
- [6] W.L. Patterson, “A Raytrace method for a laterally heterogeneous environment,” *NOSC TR.*, No. 1180, July 1987.
- [7] R.H. Hardin and F.D. Tappert, “Application of the split-step Fourier method to the numerical solution of nonlinear and variable coefficient wave equations,” *SIAM Rev.*, vol. 15, p 423, 1973.
- [8] H.V. Hitney, “Hybrid Ray Optics and Parabolic Equation Methods for Radar Propagation Modeling,” in *Radar '92 IEE Conf. Pub. 365*, 12-13 Oct 1992, pp. 58–61.
- [9] A.E. Barrios, “Advanced Propagation Model,” *Proc. Of the 1997 Battlespace Atmospherics Conf.*, NRaD TD 29892-4 Dec 1997, pp. 483–490.
- [10] A.E. Barrios, “A Terrain Parabolic Equation Model for Propagation in the Troposphere,” *IEEE Trans. On Ant. And Prop.*, vol. 42, no. 1, pp. 90–98, Jan. 1994.
- [11] J.R. Kuttler and G.D. Dockery, “Theoretical description of the parabolic approximation/Fourier split-step method of representing electromagnetic propagation in the troposphere,” *Radio Sci.*, vol. 26, pp 381–393, 1991.
- [12] D.J. Donohue and J.R. Kuttler, “Propagation Modeling over Terrain Using the Parabolic Wave Equation,” *IEEE Trans. On Ant. And Prop.*, vol. 48, no. 2, pp 260–277, Feb. 2000.
- [13] H.R. Reed, and C.M. Russell, *Ultra High Frequency Propagation*, Boston Technical Publishers, Inc. Cambridge, MA, USA 1966
- [14] G.D. Dockery and J.R. Kuttler, “An Improved Impedance-Boundary Algorithm for Fourier Split-Step Solutions of the Parabolic Wave Equation,” *IEEE Trans. On Ant. And Prop.*, vol. 44, no. 12, pp 1592–1599, Dec. 1996.
- [15] J.R. Kuttler, “The Forward, Backward and Central Difference Algorithms for Implementing Mixed Fourier Transforms to Improve TEMPER”, APL Report A2A-00-U-0-010, Aug. 2000.
- [16] A.E. Barrios, “Terrain and Refractivity Effects on Non-Optical Paths”, AGARD EPP Symposium on Multiple Mechanism Propagation Paths: Their Characterisation and Influence on System Design, 4-8 Oct. 1993, pp. 10-1 - 10-9.
- [17] LCDR R. O’Carroll, AGC(SW) J. Deunger, AGC(SW) M. Duensing, and AGC(SW) P. Rossman, “Operational Analysis of Radar Propagation Over Terrain (RPOT),” *Proc. EM/EO Prediction Requirements & Products Symp.*, June 1997, pp 33-38.